



# High stability in near-infrared spectroscopy: part 1, adapting clock techniques to optical feedback

Mathieu Casado<sup>1,2,3</sup> · Tim Stoltmann<sup>1,4</sup> · Amaelle Landais<sup>2</sup> · Nicolas Jobert<sup>5</sup> · Mathieu Daëron<sup>2</sup> · Frederic Prié<sup>2</sup> · Samir Kassi<sup>1</sup>

Received: 27 April 2021 / Accepted: 21 January 2022

© The Author(s), under exclusive licence to Springer-Verlag GmbH Germany, part of Springer Nature 2022

## Abstract

Optical feedback is an efficient way to narrow and stabilise semi-conductor lasers. As a step forward for ultra-stable, yet highly tunable sources, we developed a new prototype of a three-mirror V-shaped optical cavity (VCOF). It is made of a precisely machined Zerodur spacer, that holds 3 optical contacted mirrors forming a high finesse V-shaped cavity. This arrangement allows the resonant light to be sent back to the seeding laser, triggering a drastic narrowing of the emission linewidth well below the cavity mode width without the need for high-bandwidth active electronic lock of the laser on the cavity. Low expansion material and precise temperature control of the reference cavity leads to a source with Hz level frequency drift and 70 Hz-level emission linewidth at 215 THz. We discuss the benefits of this new prototype compared to its predecessor for high-sensitivity cavity ring down spectroscopy (CRDS). To serve this purpose, the frequency stabilised laser was characterised on short, mid and long time scales, using a high finesse etalon, a self referenced optical frequency comb and a long term saturated CRDS absorption Lamb dip measurement on water.

## 1 Introduction

Laser absorption spectroscopy is a widely used method for fast and precise trace detection measurements in gas [1, 2]. Narrow and stable (in term of frequency deviation) laser sources are crucial to reach the precision and accuracy requirements of high-precision spectroscopy, that have increased in the past years [3]. In particular, to achieve performances capable to distinguish different isotopes of the same molecule (such as water or carbon dioxide, relevant for environmental studies), extreme sensitivity levels are required [4–7]. The traditional continuous wave cavity ring

down spectroscopy (cw-CRDS) [8, 9] relies on the coupling of a resonator with a mono-frequency laser. While for a single ring-down, the resonator maintains a fixed, high finesse frequency, the coupling of the resonator with the seeding light prevents an accurate determination of the frequency axis, and in turn, limit the precision of the spectroscopic measurement. One way to stabilise a laser source is to remove the jitter of the laser with Pound-Drever-Hall (PDH) lock technique [10, 11] that actively locks the laser frequency on a cavity, usually linear. It is common to use the CRDS cavity itself as a resonator to achieve efficient stabilisation of a free-running laser (FARS CRDS [12]). This locking scheme requires the laser source to have an already quite low frequency noise and is generally limited to expensive, and complex to drive tunable External Cavity Diode Laser [13] or poorly tunable pre-stabilised laser [14]. On the other hand, widely available distributed feedback laser diode (DFB) are rather broadly and easily tunable but suffer a high jitter noise, leading to MHz emission linewidth.

Optical feedback is an elegant method to improve the spectral properties of lasers such as distributed feedback diodes (DFB) [15]. The long term stability of an external reference cavity is transferred via direct optical feedback to the seeding laser, whose emission linewidth is narrowed well below the mode width of the seeded cavity. This well

✉ Mathieu Casado  
mathieu.casado@gmail.com

<sup>1</sup> LiPHY, Laboratoire Interdisciplinaire de Physique, Université Grenoble Alpes/CNRS, 38000 Grenoble, France

<sup>2</sup> Laboratoire des Sciences du Climat et de l'Environnement, LSCE/IPSL, CEA-CNRS-UVSQ, Université Paris-Saclay, Gif-sur-Yvette, France

<sup>3</sup> Present Address: Alfred Wegener Institut Helmholtz Centre for Polar and Marine Research, Postdam, Germany

<sup>4</sup> Present Address: AP2E, Aix en Provence, France

<sup>5</sup> ALMA Consulting, Arcueil, France

understood mechanism [16] has been exploited in Optical Feedback Cavity Enhanced Absorption Spectrometer (OFCEAS) setups [17], in fibre Bragg gratings [18] and V shaped Cavity Optical Feedback laser sources (VCOF) [15]. V-shaped cavities are classically used to avoid unwanted feedback from the reflection of the entry mirror, making it straightforward to obtain high level optical feedback from the cavity by only controlling the feedback phase with a slow PID servo loop (8 kHz bandwidth), acting on either a mirror actuated by piezoelectric or an electro-optic phase modulator (patented technology FR3056837B1). The linewidth and the stability of the laser are therefore linked to the thermo-mechanical properties of the cavity used for the optical feedback. In order to improve the thermal stability and the mechanical stiffness of the V-shaped cavity compared to previous models [15], and following classical designs of cavities made for atomic clocks [19, 20], we used a monobloc Zerodur cavity on which the mirrors are optically contacted (see Fig. 1). As a result, the laser spectral purity and long term frequency stability were increased, even though without reaching atomic cavity stability level due to a sub-optimal, but very competitively priced, design.

Moreover, this cavity is seeded by a fibred DFB laser (modified Eblana EP1392-DM), demonstrating for the first time that optical feedback can be achieved through fibred system (patented technology FR3056837B1). These developments have been pushed forward in order to facilitate the development of narrow and stable laser sources for near-infrared spectroscopy instruments. This particular set-up goes beyond the specifications required for an infrared spectrometer, as a result, it has enabled us to identify the limits both from an optical point of view and thermo-mechanical considerations.

## 2 Experimental setup

We have designed a robust V-shaped monolithic spacer, optically contacted with 3 spherical mirrors, aiming at improving the long term stability of previous realisations [6, 15] and inspired by cavity designs of atomic clocks. The cavity is made of a Zerodur glass with thermal expansion coefficient of  $7.10^{-9} K^{-1}$ . The internal cavity length is 18.43 cm and has a free spectral range of  $c/4L \approx 406 MHz$  due to the two fold geometry. The cavity was assembled using mirrors with a reflectivity at 1390 nm of 0.999977. The finesse of the cavity is thus 131000 and the intra-cavity photon lifetime is 24.1  $\mu s$ . By tuning the laser temperature from  $-10^\circ C$  to  $60^\circ C$ , we could lock the laser over 2658 successive cavity modes, spanning over more than 1 THz (see Fig. 2). We deduced a V-shaped cavity free spectral range (FSR) of  $406337674.5 \pm 0.3 Hz$ . This effective cavity length includes the first order dispersion due to the cavity mirrors [21]. With

a flat linear fit residual (Fig. 2, upper panel) over the 1 THz explored region, no sign of second order dispersion was evidenced.

The agility of the laser source is also demonstrated in a scan of the frequency of the DFB laser by changing its temperature (Fig. 2 bottom right panel): the laser remains locked over a broad spectral region (locking range), until it delocks, being pushed too far from the resonant mode. In our experiment, we only scanned the temperature of the DFB, and as soon as the laser emission approaches the cavity modes, the automatic relock occurs, in the present setup, within a few hundreds of millisecond. The agility of the relock is not limited to slow scans, and similar performances can be achieved jumping a large number of modes (in this case, only limited by the response time of the DFB laser to temperature changes).

In order to limit thermal effects, the cavity is surrounded by a 5 mm thick copper shield damping the external temperature excursion. Moreover, the assembly is housed in a stainless steel vacuum enclosure pumped down to  $10^{-8} mbar$  by a vibration-free ionic pumping system. Three wedged optical ports with anti-reflection coatings (two on the top and one on the bottom flange) allow the light to enter or exit the assembly. Note that a single window allows two beams to be extracted through the bottom flange, corresponding to the laser injection and feedback port.

As illustrated in Fig. 1, the V-shaped cavity is seeded using a modified fibred DFB laser Eblana EP1392. By using polarisation maintaining fibres, optical feedback is achieved as straightforwardly as with a free space diode. This technique, already used in fibre gratings [18], was never successful for external cavities and relies on the combined use of polarisation maintaining fibres, the absence of optical isolator in front of the laser, and active phase correction. The laser-cavity distance is controlled using a fibred Electro-Optic Modulator (EOM) taking into account slow phase drifts of the feedback path length. Practically, we apply a weak 50kHz modulation to the EOM to determine with the help of a lockin amplifier the relative phase between the laser and the cavity [15]). We have evaluated the performance of this new optical feedback laser source by combining several optical setups to evaluate the spectral properties over time scales from the ms to several days. The most straightforward approach to evaluate the performances of the system would be to do a beatnote with two replicates laser sources which could not be achieved. Instead, we use several approaches allow for precise frequency measurement at both short and long time scales. Commercial wavemeters are limited to an accuracy of a few MHz over a limited period (hours), which makes them too inaccurate for an extensive characterization, but permits to unambiguously identify which V cavity mode is acting. Nevertheless, in combination with the beatnote obtained by mixing the laser with a GPS-referenced optical

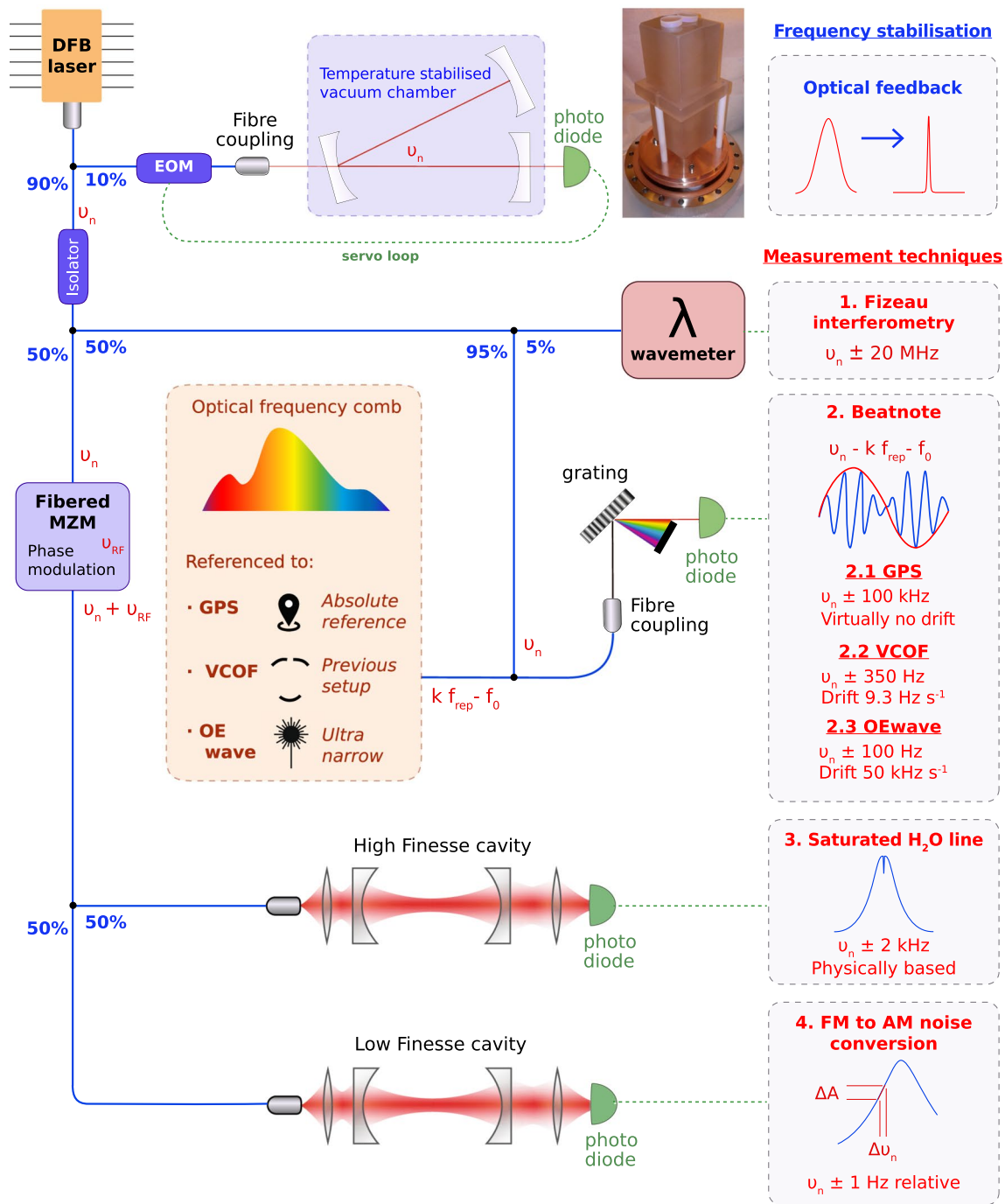


**Fig. 1** Presentation of the experimental setup used to measure the frequency to characterise the cavity: 1. Fizeau interferometry is a common method to obtain rough estimates of frequency using interference features, 2. the beatnote uses the frequency modulation with

another known frequency, 3. saturated absorption is using the narrow spectral signature of saturation of an absorption transition, and 4. FM to AM noise conversion is using frequency to amplitude noise conversion on the side of a low finesse optical etalon resonance

frequency comb (MENLO FC1500), determination of the absolute frequency can be refined down to a few Hz (measurement technique 2.1. in Fig 1) [22]. In Fig. 3 the frequency deviation of the DFB laser stabilised against the optically contacted cavity (red curve) is presented in comparison

with a range of commercial tunable lasers (the grey area encompasses the temperature stabilised DFB diode, top edge, and the free-running ECDL, bottom edge). Without optical feedback, DFB laser sources are typically MHz broad and start drifting within 100 ms. For a room temperature

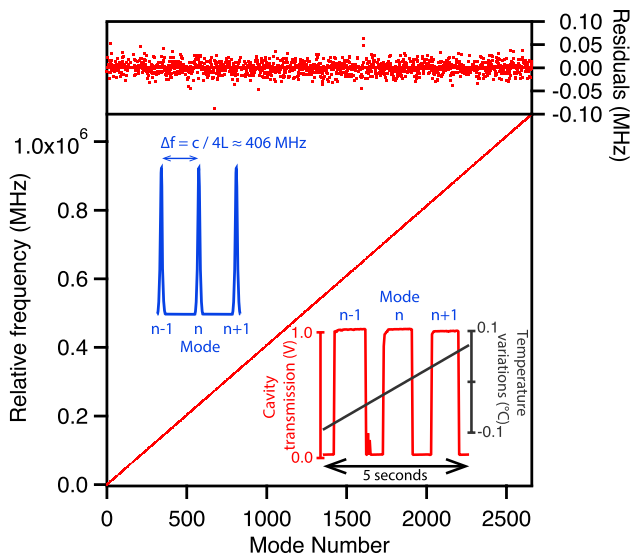


**Fig. 2** Free spectral range estimated using the beatnote with the comb (method 2.1). The standard deviation of the measurement is roughly  $10\text{ kHz}$  due to the wide linewidth of the comb teeth compared to the VCOF. Top left insert: illustration of the FSR of the cavity; bottom right insert: temporal zoom on the laser locking on successive mode while the temperature is scanned, the relock is instantaneous

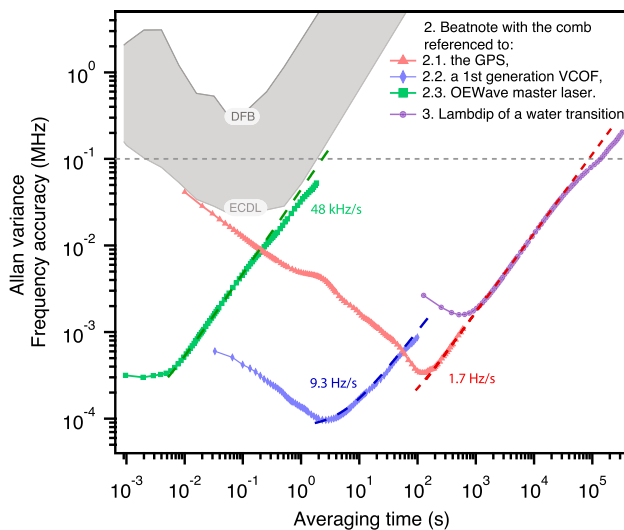


**Fig. 3** Comparison of the Allan variance of the frequency of a DFB locked on the VCOF measured by the beatnote with a tooth of the comb locked on 2.1 a GPS (red triangles), 2.2 a first generation VCOF (blue diamonds), 2.3 an OEwave laser (green squares) or by using the center of a Lamb dip of a saturated absorption (method 3, purple). The grey area illustrates the range of stability for common tunable laser sources (top, DFB laser, bottom, ECDL)

and free-running ECDL (among the narrow widely tunable laser sources), we can see that the Allan variance decreases down to  $20\text{ kHz}$  after  $0.1\text{ s}$  before thermomechanical drifts take over (bottom grey curve in Fig. 3). For the DFB laser locked on the VCOF, we observe that the Allan variance

decreases following a  $N^{-1/2}$  ergodic law. A minimum deviation of  $341\text{ Hz}$  is reached after  $110\text{ s}$ . The rising slope of  $1.7\text{ Hz}\cdot\text{s}^{-1}$  observed after  $110\text{ s}$  gives an estimate of the long term drift of the cavity. It is about 10 times more stable than the previous generation of VCOF [15].

### 3 Frequency deviation

One of the measurement limits here is that the linewidth of each tooth of the GPS disciplined optical frequency comb (OFC) is intrinsically much larger than the VCOF emission linewidth, leading to an apparent noise excess of  $100\text{ kHz}$ . To overcome this limitation, we have repeated the measurement with the OFC being optically locked to a VCOF of a previous generation (measurement technique 2.2. in Fig 1), similar to the one in the study of [15]. We obtained an increased combined drift ( $9.3\text{ Hz}\cdot\text{s}^{-1}$ ), but a much lower short-time combined noise ( $600\text{ Hz}$ ) and a lower variance minimum ( $96\text{ Hz}$ ), confirming the ability of VCOF cavities to be used for determining frequencies with a precision better than  $100\text{ Hz}$  within one second (blue curve 2.2 in Fig. 3). Due to its composite mechanical structure, the old VCOF setup was prone to frequency noise, which was stated to be on the order of  $600\text{ Hz}$  [15]. We thus estimate that the short-time combined noise is dominated by the old VCOF setup short term noise.

In order to confirm this hypothesis, the OFC was locked to a narrow linewidth commercial laser OEwave (measurement technique 2.3. in Fig 1). We obtained a short term combined noise of  $317\text{ Hz}$  but a fast  $48\text{ kHz}\cdot\text{s}^{-1}$  drift of the Allan variance curve (green trace in Fig 3). The flat Allan variance during the first  $10\text{ ms}$  indicates that noise from one of the lasers is dominating. Considering that the blue trace goes below  $100\text{ Hz}$ , one concludes that the OEwave is responsible for the drift. Since in experiment 2.2, the OFC was locked at  $1550\text{ nm}$  while the VCOF emission is at  $1400\text{ nm}$ , part of the short term noise may be due to incomplete coherence transfer from tooth to tooth [23]. One may conclude that the short term noise excess of the old VCOF version is between  $300$  and  $600\text{ Hz}$  (blue curve), and that the one of the new VCOF is below  $300\text{ Hz}$ . For the drifts, we put forward that the OEwave, Old VCOF and new VCOF drift by about  $50\text{ kHz}\cdot\text{s}^{-1}$  (green curve),  $10\text{ Hz}\cdot\text{s}^{-1}$  (blue curve) and  $2\text{ Hz}\cdot\text{s}^{-1}$  (red curve), respectively.

To confirm the results, another method was used to independently assess these performances: we carried out an Allan Variance study of the VCOF drift monitoring a molecular absorption line. We recorded a Lamb dip feature of a strong water line over several days [22]. The Lamb dip [22, 24] is a narrow peak that shows up at the center of the Doppler limited absorption (measurement technique 3. in

Fig 1). It has a sufficiently narrow signature to allow for a centre determination with  $2\text{ kHz}$  frequency accuracy. This is presented in purple in Fig. 3. Lamb dip measurements provide an independent measurement of the long term behaviour of the cavity and confirm drift level below  $2\text{ Hz}\cdot\text{s}^{-1}$ . Note that the drift of the cavity length (and in turn of the frequency) is not monotonous over a timescale on the order of a day, but oscillates around an equilibrium position. Thus, over several days, the frequency deviations are limited to  $100\text{ kHz}$ , leading to a drift below  $0.3\text{ Hz}\cdot\text{s}^{-1}$  for time scales longer than  $10^5\text{ s}$ . This was confirmed by a two-year regular monitoring of the Lamb dip feature indicated that the aging of the assembly was  $0.73 \pm 0.09\text{ Hz}\cdot\text{s}^{-1}$ , typical for Zerodur assemblies [25].

As a final attempt to evaluate the intrinsic noise of the cavity, we injected the laser in a relatively low finesse cavity (approximately 13500), used as a frequency etalon (measurement technique 4. in Fig 1). Indeed, at the half-maximum of the transmission peak of the low finesse cavity, the variation of the transmission with the laser optical frequency is locally linear ( $r^2 = 0.98$ ). As a result, the frequency noise of the injected light is converted in transmitted power variations (see Fig. 4). Obviously, this method is limited by the thermomechanical fluctuations of the etalon cavity length that shifts its resonant frequency and the 10 m long unstabilised fibre link from the VCOF to the cell [26, 27]. A typical transmitted power trace is given in Fig. 4. The raw data (grey curve, right panel) includes the high-frequency modulation applied to maintain the laser light locked to the VCOF (see Section 2). This high-frequency modulation ( $50\text{ kHz}$ ) can be filtered out to obtain the actual intrinsic noise of the light produced by the V-shaped cavity.

We observe that the standard deviation of the frequency excursion is  $913\text{ Hz}$ , once the modulation implemented to

lock the laser source in the low finesse etalon has been filtered. This value is larger than expected considering the finesse of the cavity, as previously mentioned. Additionally, there seems to be a narrower structure inside the relatively slow oscillations observed in the time series. Assuming the large excursions are due to the etalon and the fibre link, which is justified according to the upper linewidth set by the green curve in Fig. 3, only a  $181\text{ Hz}$  RMS excursion would be associated with the VCOF, as shown in the zoom part (red inset).

Using the beta-separation line technique [28], we estimate which part of the noise is linked to the intrinsic noise of the VCOF (below  $70\text{ Hz}$ , blue area in Fig. 5) and contributes

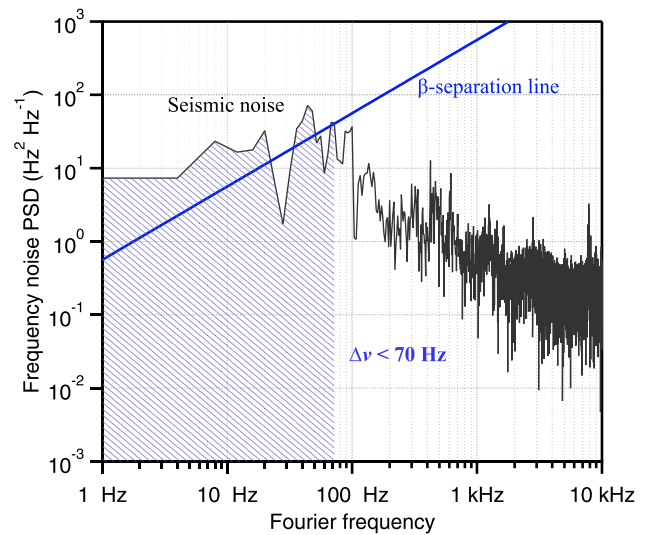


Fig. 5 Frequency noise PSD of the VCOF with a frequency etalon. The shaded area A corresponds to a laser linewidth  $\Delta\nu = \sqrt{8 \ln 2 A}$  [15, 28]

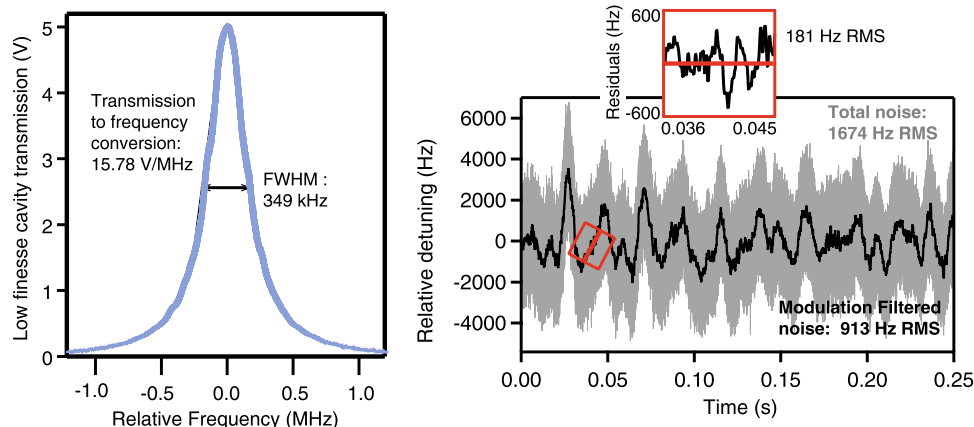
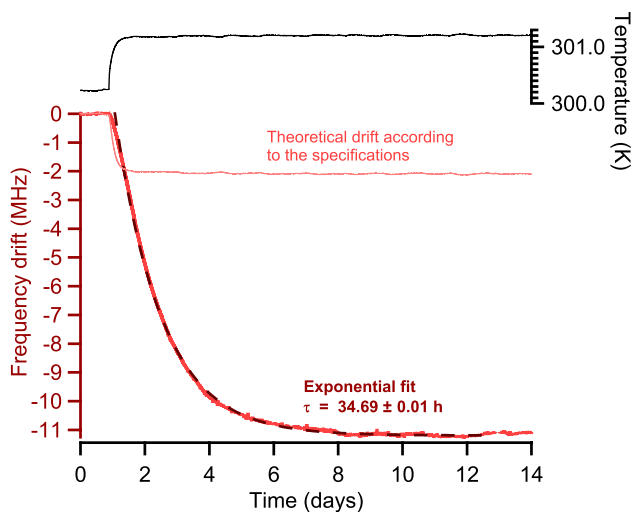


Fig. 4 Evaluation of the linewidth of the VCOF with a low finesse etalon: left, scan of the etalon transmitted power over  $2.4\text{ MHz}$ , right, relative detuning of the VCOF obtained by converting the power fluctuation into frequency fluctuation with a slope of  $15.78\text{ V MHz}^{-1}$  (raw

conversion, grey curve), filtering the high-frequency modulation used to lock the cavity (low-pass filtered, black curve), and zooming on the sub-structure associated solely with the VCOF frequency variation (red inset)



**Fig. 6** Evaluation of the drift of the cavity for a temperature shift of 1 K: time series of the temperature on the external flange (black line), frequency drift measured by beatnote with the OFC (red thick line), exponential fit of the variations (dark red dashed line), and expected drift according to the specifications of the Zerodur spacer (light red line)

to the laser linewidth, and which part of the noise does not contribute to the linewidth (more than 100 Hz). As for [15], the laser frequency noise is most likely to be lower than what we obtain here as we combine the noise of both the etalon and the VCOF. These results suggest that the laser full width at half-maximum (FWHM) is below 70 Hz, almost one order of magnitude narrower than the previous VCOF [15], narrowing by more than four orders of magnitude the DFB laser used as a source. While this figure is much larger than what is presently achieved by atomic clocks or some commercial lasers such as the EOWave, combined with a very low drift and a tunability across several THz, this source reaches unique performances that, for instance, enable to study hyperfine structures within molecular transition [22], and thus provide a referenced laser source that can be used for optical spectroscopy out of a laboratory.

Overall, the vibrational study [29] predicts that at this time scale, the frequency excursions of the VCOF should be within 10 to 100 Hz, which concurs with our experimental results. On the other hand, the drift predicted by the mechanical study carried out for this setup, mainly aging and temperature fluctuations, are expected to be smaller than observed. To evaluate the temperature sensitivity of the cavity, we proceeded to an abrupt temperature step of 0.96 K of the regulation box setpoint (normally temperature controlled within 10 mK). Figure 6 indicates that the frequency response of the cavity (around 11 MHz) is much larger than expected from the Zerodur thermal expansion coefficient (around 2 MHz). This can be partly explained by thermally-induced stress deforming the mirror curvature,

and subsequently affecting the resonance frequencies of the cavity modes [29]. Note that the introduction of a massive copper shield introduced a much longer response time (almost 36 hours) of the system to external temperature fluctuations than for the previous system. Coupled with the higher performances of the cavity (11 MHz/K against more than 100 MHz/K for previous generations [15]), this leads to low level of drift, and thus this system does not require routine frequency referencing. In particular, combined with active temperature stabilisation of the vacuum enclosure (within 10 mK), the frequency drift of the cavity remains below  $2 \text{ Hz s}^{-1}$  even if the temperature stabilisation of the environment exceed 1 K, with maximum daily excursion around 50 kHz. As such, it is therefore a big step towards field-deployable very narrow, yet broadly tunable, laser sources, that should fulfil requirements for most field spectroscopy campaign purposes.

## 4 Conclusion

To sum up, we have characterised a new iteration of a V-shaped Cavity stabilising a laser by Optical Feedback, with very stable frequency stability (below  $2 \text{ Hz} \cdot \text{s}^{-1}$ ), a very narrow linewidth (below 100 Hz), and high power efficiency (more than 80% of the light being available for applications). The Optical Feedback was achieved through fibre coupling. The laser-cavity optical distance was controlled with a fibred electro-optic phase modulator (EOM) acting as an optical distance modulator. In addition to the DC correction signal, a low-excursion 50 kHz modulation was applied to the EOM. This induced a modulated transmission signal that was used to infer the DC correction to be applied by the servo loop in order to keep the laser and the cavity at the ideal optical cavity, modulo  $2\pi$ . Finally, this enables to obtain rapid (less than 100 ms to lock) and stable through time (the laser can remained locked without adjustments) optical feedback on the DFB diode.

This new laser source is intended to be used for high precision spectroscopy (for example to be injected into a CRDS cavity [6, 30]), or even in laboratories not equipped with a comb to measure absolute frequency. In the field, making use of the low drift value, and measuring the Lamb dip of a known transition, this temperature stabilised laser source can be used as a frequency reference. Alternatively, coupled to an optical frequency source, it can be used to retrieve accurate optical frequencies or improve the comb linewidth to transfer its high coherency to sources over a large range of wavelengths [23].

**Acknowledgements** The research leading to these results received funding from the European Research Council under the European Union's Seventh Framework Programme (FP7/2007-2013)/RC grant

agreement number 306045, from the Agence Nationale de la Recherche (Grant ANR-13-JS060005), from Institut National des Sciences de l'Univers (LEFE/CHAT), from the Alexander von Humboldt foundation project DEAPICE. The authors acknowledge the technical support of Arnaud Dapoigny, David Terrier, Damien Capolongo and Hugues Guillet de Chatellus. The Zerodur spacer was built by Winlight Optics.

## References

1. P. Werle, *Spectrochim. Acta Part A Mol. Biomol. Spectrosc.* **54**(2), 197 (1998)
2. E. Kerstel, L. Gianfrani, *Appl. Phys. B* **92**(3), 439 (2008)
3. J.M. Hartmann, H. Tran, R. Armante, C. Boulet, A. Campargue, F. Forget, L. Gianfrani, I. Gordon, S. Guerlet, M. Gustafsson, J.T. Hodges, S. Kassı, D. Lisak, F. Thibault, G.C. Toon, *Spectrosc. Radiat. Transf.* (2018)
4. J. Landsberg, D. Romanini, E. Kerstel, *Opt. Lett.* **39**(7), 1795 (2014). <https://doi.org/10.1364/OL.39.001795>
5. E.J. Steig, V. Gkinis, A.J. Schauer, S.W. Schoenemann, K. Samek, J. Hoffnagle, K.J. Dennis, S.M. Tan, *Atmos. Meas. Tech.* **7**(8), 2421 (2014). <https://doi.org/10.5194/amt-7-2421-2014>
6. T. Stoltmann, M. Casado, M. Daëron, A. Landais, S. Kassı, *Anal. Chem.* **89**(19), 10129 (2017)
7. M. Casado, Water stable isotopic composition on the East Antarctic Plateau: measurements at low temperature of the vapour composition, utilisation as an atmospheric tracer and implication for paleoclimate studies. Ph.D. thesis, Paris Saclay (2016)
8. D. Romanini, P. Dupre, R. Jost, *Vib. Spectrosc.* **19**(1), 93 (1999)
9. P. Macko, R. Plašil, P. Kudrna, P. Hlavenka, V. Poterya, A. Pysanenko, G. Bánó, J. Glosik, *Czechoslov. J. Phys.* **52**(2002 Suppl D), D695 (2002)
10. R.V. Pound, *Rev. Sci. Instrum.* **17**(11), 490 (1946)
11. R.W.P. Drever, J.L. Hall, F.V. Kowalski, J. Hough, G.M. Ford, A.J. Munley, H. Ward, *Appl. Phys. B* **31**(2), 97 (1983)
12. G.W. Truong, K.O. Douglass, S.E. Maxwell, R.D. van Zee, D.F. Plusquellic, J.T. Hodges, D.A. Long, *Nat. Photon.* **7**, 532 (2013)
13. J.T. Hodges, R. Ciuryło, *Rev. Sci. Instrum.* **76**(2), 23112 (2005)
14. V. Crozatier, F. De Seze, L. Haals, F. Bretenaker, I. Lorgeté, J.L. Le Gouët, *Opt. Commun.* **241**(1–3), 203 (2004)
15. J. Burkart, D. Romanini, S. Kassı, *Opt. Lett.* **38**(12), 2062 (2013)
16. P. Laurent, A. Clairon, C. Breant, *IEEE J. Quantum. Electron.* **25**(6), 1131 (1989)
17. J. Morville, S. Kassı, M. Chenevier, D. Romanini, *Appl. Phys. B* **80**(8), 1027 (2005). <https://doi.org/10.1007/s00340-005-1828-z>
18. F. Wei, F. Yang, X. Zhang, D. Xu, M. Ding, L. Zhang, D. Chen, H. Cai, Z. Fang, G. Xijia, *Opt. Express* **24**(15), 17406 (2016)
19. A.D. Ludlow, X. Huang, M. Notcutt, T. Zanon-Willette, S.M. Foreman, M.M. Boyd, S. Blatt, J. Ye, *Opt. Lett.* **32**(6), 641 (2007). <https://doi.org/10.1364/OL.32.000641>
20. J. Millo, D.V. Magalhaes, C. Mandache, Y. Le Coq, E.M.L. English, P.G. Westergaard, J. Lodewyck, S. Bize, P. Lemonde, G. Santarelli, *Phys. Rev. A* **79**(5), 53829 (2009)
21. L. Rutkowski, A.C. Johansson, G. Zhao, T. Hausmaninger, A. Khodabakhsh, O. Axner, A. Foltynowicz, *Opt. Express* **25**(18), 21711 (2017)
22. S. Kassı, T. Stoltmann, M. Casado, M. Daëron, A. Campargue, *J. Chem. Phys.* **148**(5), 54201 (2018). <https://doi.org/10.1063/1.5010957>
23. R. Gotti, T. Sala, M. Prevedelli, S. Kassı, M. Marangoni, D. Romanini, *J. Chem. Phys.* **149**(15), 154201 (2018). <https://doi.org/10.1063/1.5046387>
24. J. Burkart, T. Sala, D. Romanini, M. Marangoni, A. Campargue, S. Kassı, *J. Chem. Phys.* **142**(19), 191103 (2015)
25. R.W. Fox, B.R. Washburn, N.R. Newbury, L. Hollberg, *Appl. Opt.* **44**(36), 7793 (2005)
26. J. Ye, Q. Li, S.Q. Peng, Y.L. Chen, *Appl. Opt.* **29**(12), 1724 (1990)
27. L.S. Ma, P. Jungner, J. Ye, J.L. Hall, *Opt. Lett.* **19**(21), 1777 (1994)
28. G. Di Domenico, S. Schilt, P. Thomann, *Appl. Opt.* **49**(25), 4801 (2010). <https://doi.org/10.1364/AO.49.004801>
29. N. Jobert, M. Casado, S. Kassı, *Appl. Phys. B* (2022). <https://doi.org/10.1007/s00340-022-07779-x>
30. J. Burkart, S. Kassı, *Appl. Phys. B* **119**(1), 97 (2015). <https://doi.org/10.1007/s00340-014-5999-3>

**Publisher's Note** Springer Nature remains neutral with regard to jurisdictional claims in published maps and institutional affiliations.